

Review

The Role of Geometric Sites in 2D Materials for Energy Storage

Yijun Yang,^{1,9} Xizheng Liu,^{2,9} Zhian Zhu,³ Yeteng Zhong,⁴ Yoshio Bando,^{5,6} Dmitri Golberg,^{5,7} Jiannian Yao,^{6,8} and Xi Wang^{1,6,*}

Two-dimensional nanostructures may effectively be utilized as electrode materials for lithium/sodium-ion batteries to enhance the energy and power densities and cycling stability, and to satisfy the increasing demands of electrical vehicles and power stations. This review introduces the “geometry-driven” concept to illuminate the mechanisms related to various geometric sites in 2D materials for improving their electrochemical performance. The geometric sites of 2D materials are categorized into point-like, line-like, and plane-like defects. The electronic structures of geometric sites are then discussed. Hierarchical materials constructed from 2D materials, such as 3D crumpled nanoparticles, nanoflowers, and heterostructures, are highlighted. A summary of applications of the *in situ* transmission electron microscopy (TEM) technique is presented toward understanding the mechanisms of geometric-site effects in 2D materials. Finally, some perspectives on the geometry concept for material designs, theoretical calculations for performance prediction, and modern *in situ* TEM techniques for uncovering electrochemical mechanisms are discussed.

Introduction

The ever-increasing demands of electrical vehicles and power station utilization promote the development of rechargeable batteries with superior electrochemical performances.^{1–7} To further enhance the energy and power densities, the design of new electrode materials with higher specific capacities, especially beyond their theoretical capacities, is desirable. Such a task is of high priority. Two-dimensional (2D) nanostructures represent a material family with various layered ensembles. These include graphene,^{8–13} transition metal dichalcogenides (TMDCs),^{14–20} phosphorene,^{21–24} g-C₃N₄,²⁵ MXenes,^{26–29} h-BN,^{30,31} and layered double hydroxides,^{32–34} among others. Most of these 2D materials, and their derivatives, have been adopted as electrodes in energy-storage devices, especially for rechargeable batteries. They indeed exhibit a superior Li/Na storage performance.³⁵ Interestingly, one of the most important features of 2D materials is their self-assembly and richness of micro-/nanostructures, which provide many more newly generated geometric sites for storage of the guest ions. This is a newly emerging discipline in regard of the required mathematical concept, materials design, and fabrication, as well as electrochemistry, which in short can be termed “geometry-driven” energy storage.^{36–38} These approaches have greatly promoted the investigation and application of 2D-based materials as electrodes in secondary batteries. The topic of “geometric sites” energy storage has witnessed a rapid development in recent years. Thus, a comprehensive review summarizing the present progress is indeed timely and warranted for a fundamental understanding and further optimization of electrode performance.

Therefore, in this review we first introduce the background and concept of geometry-driven energy storage and then summarize the typical materials with specific

Context & Scale

Two-dimensional (2D) materials, with unique chemical and electronic properties, have attracted great attention as one of the most promising electrode materials for rechargeable batteries to satisfy the ever-increasing demands of higher power and energy density, superior rate performance, and long cycling life. Hundreds of 2D materials and their derivatives, such as graphene, h-BN, g-C₃N₄, phosphorene, MoS₂, and MXenes, have been fabricated and utilized as electrode materials. Creating new geometric defects within 2D nanosheets and constructing three-dimensional hierarchical materials made of such sheets have been proved to be an effective strategy to further improve the electrochemical performances. This is a newly emerged discipline combining the mathematical concept, i.e., geometry, materials design engineering, and electrochemistry, which can be referred as a novel “geometry-driven” energy storage.

In this review, geometric sites of 2D materials are categorized into point-like (vacancy, protrusion, and heteroatom doping), line-like (edges, wrinkles, and lattice), and plane-like (interlayer spacing)



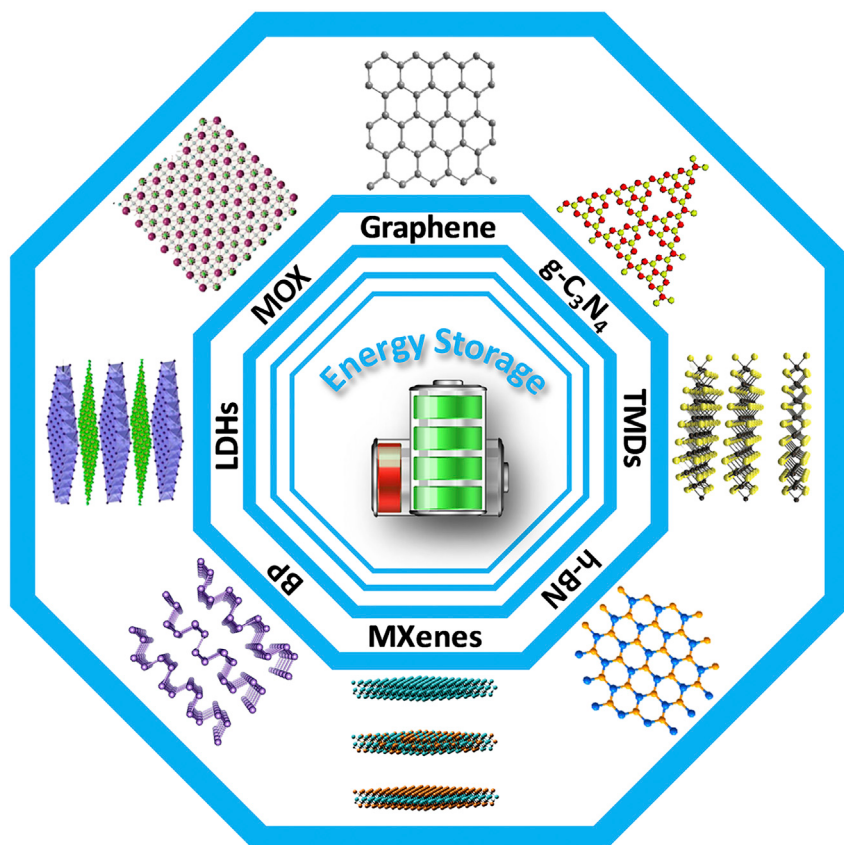


Figure 1. Schematic Illustration of 2D Materials Application for Energy Storage

barrier of 2D materials to facilitate the Li/Na transport to achieve superior rate performance. In this section, the nanogeometric sites in 2D materials, such as point-like, line-like, and plane-like, are discussed (as shown in Figure 2) based on theoretical calculations and experimental analysis. The accompanying enhanced specific capacity, high rate performance, and long cycle life are also highlighted. The three-dimensional (3D) hierarchical structure derivatives constructed from a 2D nanomaterial with novel geometric sites and chemical/physical functionalities for battery electrode materials are then summarized.

Point-like Geometric Sites in 2D Materials

Special nanogeometric structures lead to electronic structure modifications of a 2D nanosheet, thus affecting the ion-diffusion dynamics during lithium/sodium insertion/desertions and, consequently, the overall performance of an electrode material.

Graphene, as the most popular 2D material with a honeycomb-like all-carbon-atom structure, has been widely utilized as anode material for rechargeable batteries. Point-type geometric sites for Li-ion adsorption on a single-layer graphene (SLG), such as Stone-Wales (SW) defects, double vacancies (DV), and extended SW defects, were investigated by Greeley's group based on first-principles analysis.⁴³ They suggest that pristine SLG, with no defects, exhibits a positive lithiation energy with increasing Li content and consequent zero capacity, while SLG with SW and DV defects of various densities have tendencies to capture Li ions with stronger

perspectives of the regarded geometry concept for a material design, theoretical calculations for performance prediction, and *in situ* TEM techniques for uncovering electrochemical mechanisms are summarized and some possible research directions proposed to smartly utilize 2D materials in the fields of energy storage.

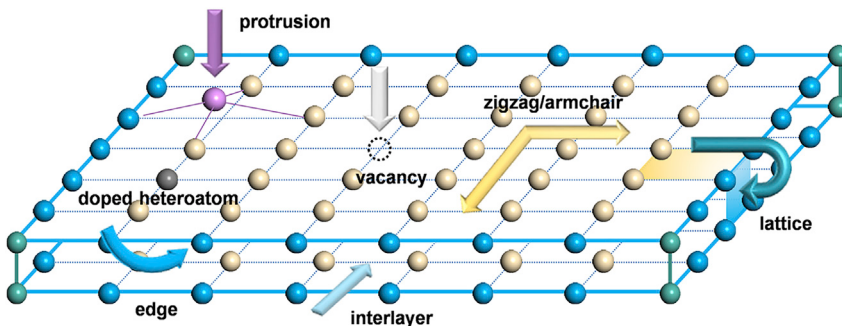


Figure 2. Schematic Illustration of Various Geometric Sites within a 2D Nanosheet: Point-like Geometric Sites (Vacancy, Protrusion, Doped Heteroatom) and Line-like Geometric Sites (Edge, Interlayer, Zigzag/Armchair, and Lattice Structures)

adsorption potential on both nanosheet sides. This consequently enhances the theoretical capacity (140 mAh g^{-1} and 160 mAh g^{-1} , respectively). Extended defects could result in line geometric defects, which bring much higher capacity (240 mAh g^{-1}). Among these defective geometric sites, the SW defect exhibits the lowest energy barrier (0.13 eV) for Li diffusion compared with other defects; this value is much lower than that for pristine graphene (0.32 eV). Chemical vapor deposition⁴⁴ and heteroatom (boron,^{45,46} nitrogen,^{47–50} sulfur,^{51–53} phosphorus,^{54–56} etc.) doping have been proved to be effective strategies to create SW defects in graphene. Furthermore, the heteroatom that substitutes for a single carbon atom also leads to a change in electrochemical properties of graphene nanosheet because of varying electronegativity of different atoms.⁵⁷ The heteroatom holey defects caused by heteroatom doping also bring about point geometric sites that affect Li/Na storage. For instance, introducing boron into graphene leads to an electron-deficient matrix and consequently stronger binding with Li ions. Monovacancy and divacancy defects induced by B-doping (Figure 3D) not only decrease the energy barrier for Li diffusion but also enhance the Li-ion adsorption and theoretical capacity.^{45,58} Experimentally, it has been confirmed that 0.88 at% boron doping in few-layered graphenes could deliver a reversible capacity of $1,549 \text{ mAh g}^{-1}$ at a current density of 50 mA g^{-1} .⁵⁹ Nitrogen doping is also a widely adopted strategy for graphene to optimize the specific capacity, because of the stronger electronegativity of nitrogen than of carbon. Pyrrolic (pentagon ring) and pyridinic (hexagon ring) nitrogen holes dug under nitrogen doping on graphene are common geometric sites (Figure 3B). Based on density functional theory (DFT) calculations of Li-ion adsorption on doped graphene, the binding energies between Li ions and pyridinic and pyridinic geometric sites are 1.37 and 1.30 eV, respectively, which are stronger than those of pristine graphene. This results in improved capacity of $1,262$ and $1,198 \text{ mAh g}^{-1}$, respectively.^{60,61} Many experimental results on nitrogen-doped graphene utilized in LIBs are consistent with these calculations. Heteroatoms with a larger diameter than carbon atom may also be introduced into graphene to create geometric sites of protrusions instead of holes. The topological defects (SW defects) of a SLG electrode introduced by Ar^+ plasma were investigated, whereby it was suggested that the density of states (DOS) of graphene and the corresponding electrical double-layer capacitance were indeed improved.⁶² The protrusions on a few-layered graphene introduced by phosphorus doping were documented by *in situ* TEM and DFT calculations (Figure 3E); for example, the phosphorus protrusion sites not only adsorb more Na ions, thus resulting in enhanced specific capacity, but also increase the metallicity of graphene during the charge/discharge processes, leading to a higher rate performance.³⁷ The holes

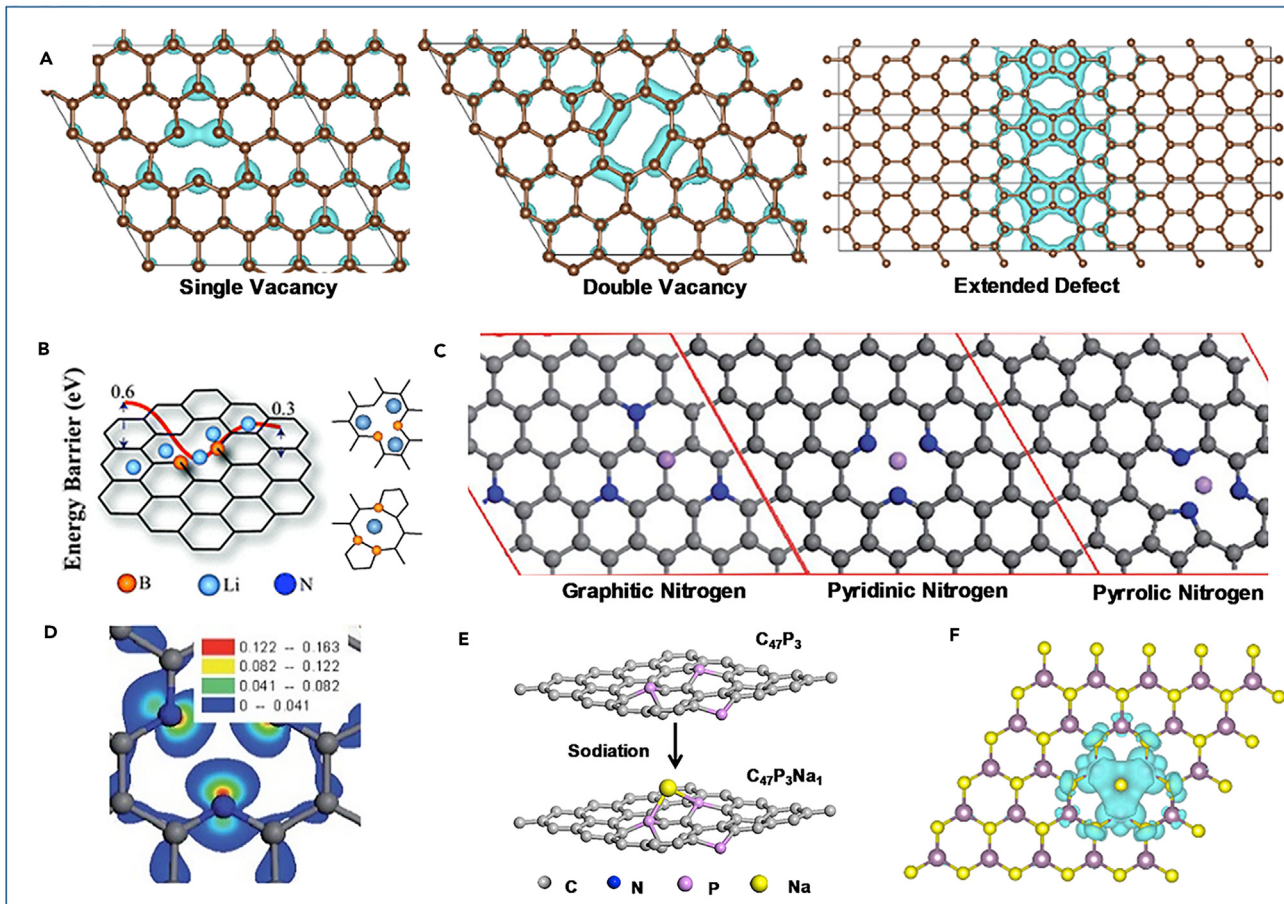


Figure 3. Point-like Geometric Sites of 2D Materials for Rechargeable Batteries

- (A) Electronic structures of a single vacancy, double vacancy, and extended defect of graphene.
 (B) The lithium-ion diffusion barrier of boron-doped graphene with two possible doping sites. Reproduced from Hardikar et al.,⁴⁵ with permission.
 (C) Three types of point nitrogen-doped graphene: graphitic, pyridinic, and pyrrolic. Reproduced from Ma et al.,⁶⁰ with permission.
 (D) The spin density distribution of pyridinic nitrogen in graphene. Reproduced from Ma et al.,⁶⁰ with permission.
 (E) Protrusion induced by phosphorus doping facilitates the enhancement of sodium-ion storage. Reproduced from Yang et al.,³⁷ with permission.
 (F) Electronic structure of MoS₂ with one sulfur vacancy.
 (A) and (F) were calculated by the density functional theory (DFT) implemented in the Vienna *ab initio* simulation package (VASP).

dug under nitrogen doping in a few-layered graphene act as Li⁺ and Na⁺ storage sites because of the lower reaction potentials.^{37,61}

MoS₂ is another promising 2D material that may be used as a negative electrode for rechargeable LIBs, since its capacity can be 1,290 mAh g⁻¹,⁶³ about 3.5 times that of commercial graphitic anodes (372 mAh g⁻¹). Sulfur vacancies in a monolayer MoS₂ nanosheet are promising geometric defects to enhance the electrochemical performance. Based on DFT simulations conducted by Liu et al.,⁶⁴ the sulfur vacancy has a formation energy of 2.35 eV in S-rich conditions, and the formation energy may decrease for E_f near the conduction band edge when the nanosheet contacts with metal, such as Li (Figure 3F). Rahman's group⁶⁵ also proved that once the sulfur vacancy is formed, it tends to be enlarged; and the longer the sulfur-vacancy row is, the more stable it becomes. A MoS₂ nanosheet with sulfur-vacancy defects would result in subcoordinated Mo centers and consequent enhanced adsorption sites for Li ions, finally improving the reversible capacity.⁶⁶

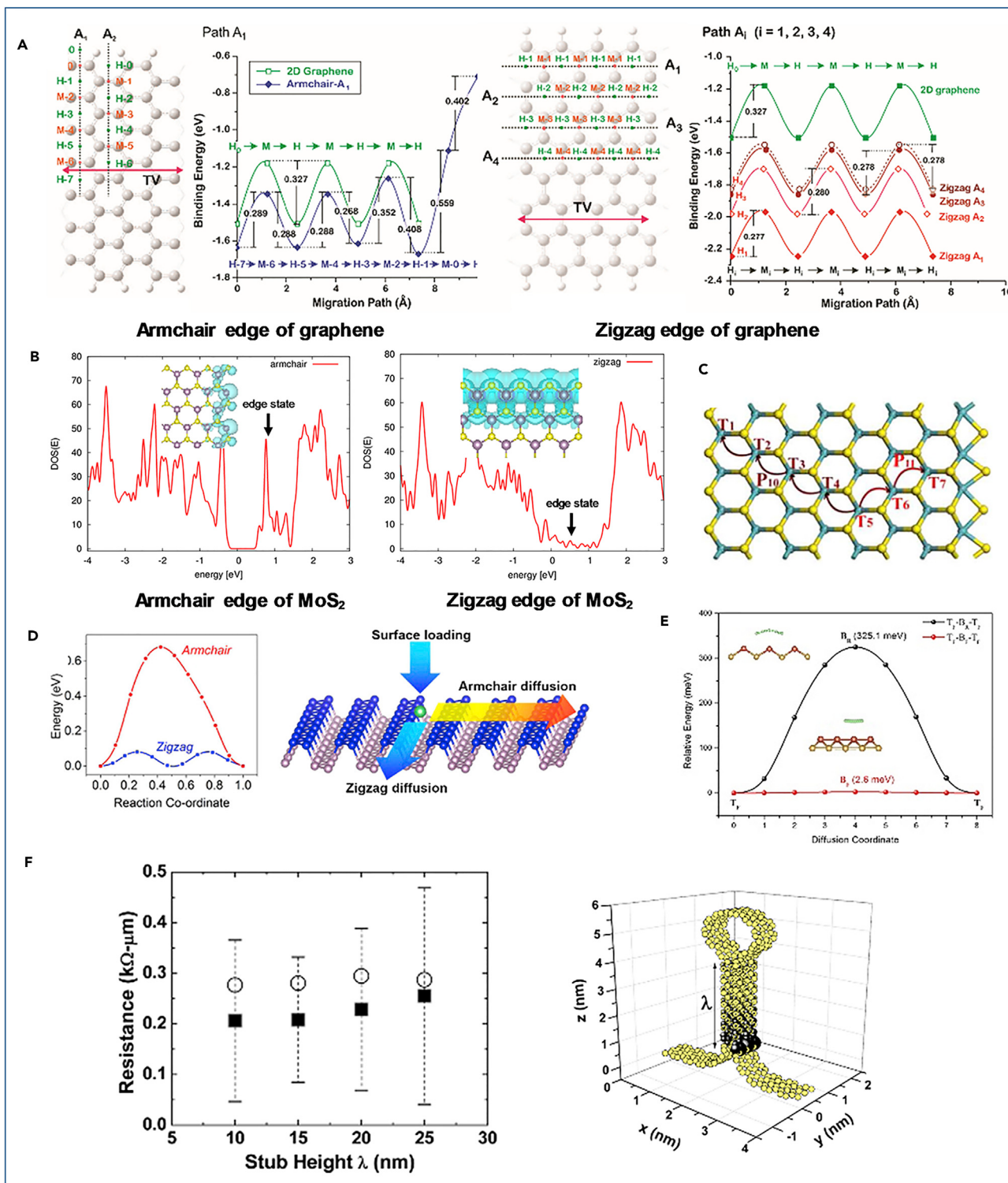


Figure 4. Line-like Geometric Sites in 2D Materials for Rechargeable Batteries

(A) Schematic representations of armchair- and zigzag-oriented graphenes and corresponding lithium-ion diffusion paths and energy barriers. Reproduced from Uthaisar and Barone,⁶⁷ with permission.

(B) DOS curves and electronic structures of armchair- and zigzag-edged MoS₂, calculated by the density functional theory implemented in the VASP.

Figure 4. Continued

(C) Schematic illustrations of two lithium-ion diffusion paths on the basal plane of zigzag-edged MoS₂ along the transverse direction. Reproduced from Li et al.,⁷⁰ with permission.

(D) Diffusion barrier curves and schematic of lithium-ion diffusion along armchair and zigzag directions of a phosphorene surface. Reproduced from Li et al.,⁷¹ with permission.

(E) Energy profile of lithium diffusion along zigzag and armchair pathways of borophene nanosheet. Reproduced from Jiang et al.,⁷² with permission.

(F) Quantum transport modeling of the room temperature resistance of a standing collapsed graphene wrinkle as a function of the collapsed bilayer length λ . Reproduced from Zhu et al.,⁷³ with permission.

Line-like Geometric Sites in 2D Materials

Line is another ubiquitous type of geometric-site defect in 2D nanosheets. Besides SW and DV defects, edges of graphene nanosheets are also of vital importance to enhance electrochemical performance.⁴² Lithium diffusion greatly depends on the adsorption and barrier energy of different planes of a 2D material, leading to anisotropic Li diffusion. For instance, the presence of edges in 2D graphene nanoribbons would create two different edges: armchair and zigzag. The adsorption and diffusion of Li ions on these two types of edges were studied by DFT calculations. Uthaisar and Barone⁶⁷ chose an isolated (4 × 4) supercell of a 2D graphene nanosheet with 32 carbon atoms, an isolated supercell of 1.58-nm wide armchair nanosheet with 56 carbon atoms with 8 hydrogen atoms passivating the edges, and an isolated supercell of 1.57-nm wide zigzag nanosheet with 64 carbon atoms and 8 hydrogen atoms passivating the edges (Figure 4A). The calculation results indicated that the presence of these edges had not only affected the reactivity of the graphene nanoribbons toward the adsorption of Li ions, but also differentiated their diffusion properties. The ions prefer to diffuse toward the edges when diffusion channels appear along the ribbon axis. For all calculated diffusion paths, the energy barriers of armchair and zigzag edges are lower (up to 0.15 eV) than those of the graphene plane, leading to a 2-fold enhancement of Li-ion diffusion coefficient at room temperature. However, such lowered diffusion barrier can only be found at a distance of a few nanometers from the edges, and creating more graphene edges can improve the diffusion coefficient and activity of Li ions within graphene.^{67–69} MoS₂ nanosheets and nanoribbons with zigzag and armchair edges were also investigated by means of DFT calculations (Figure 4B). The DOS data indicate that the armchair edge of MoS₂ is metallic, which is beneficial for Li-ion diffusion, while the zigzag edge of MoS₂ exhibits poor conductivity. Comprehensive calculations conducted by Chen et al.⁷⁰ compared the adsorption and diffusion of Li ions on 2D MoS₂ nanosheets, zigzag-edged MoS₂ nanoribbons, and MoS₂ bulk. These indicated that the ion diffusion can be improved with MoS₂ dimensionality decrease. The Li-binding energy of 2D MoS₂ nanosheets is much lower than that of MoS₂ bulk, whereas such energy for zigzag-edged MoS₂ nanosheets (with plenty of zigzag edges) exhibits the best values for fast Li diffusion (Figure 4C). Based on this, zigzag-edged MoS₂ may be the most promising MoS₂ electrode material for LIBs with high power densities and superior rate performance. Xie et al.⁴¹ experimentally reported a novel strategy to controllably fabricate MoS₂ ultrathin nanosheets with multiple edges. These allowed for exposure of more active sites and consequently enhanced the electrochemical performance.

Different from graphene nanosheets with isotropic sp² hybridization of carbon atoms and anisotropic MoS₂, phosphorene creates a puckered structure with phosphorus atoms arranged in a honeycomb lattice. Each phosphorus atom is connected to two adjoining atoms in the same plane and with one phosphorus atom in a different plane. These play an important role in Li-ion diffusion on the nanosheet surface.^{74,75} For a phosphorene monolayer, the energy barrier for Li-ion diffusion along the zigzag direction is 0.08 eV, which is much lower than that along the armchair

direction (0.68 eV, shown in [Figure 4D](#)) and is also lower than the corresponding values for MoS₂ (0.25 eV) and graphene (0.327 eV).⁷¹ The average voltage of Li-ion intercalation into a layered phosphorene was calculated to be 2.9 eV, suggesting that a phosphorene monolayer should be a promising anode material with high capacity and rate performance for batteries. Borophene, with a buckled structure similar to that of phosphorene, is proven as a promising electrode material for lithium/sodium-ion storage (1,860 mAh g⁻¹ for Li⁺⁷² and 1,218 mAh g⁻¹ for Na⁺⁷⁶). Furthermore, the energy barrier for Li-ion diffusion along the zigzag direction of monolayer borophene is 0.0026 eV, which is much lower than that of phosphorene, while the Li-ion diffusion along the armchair direction is 0.325 eV, showing the anisotropic properties ([Figure 4E](#)).

Wrinkles are formed because of protrusions or strains in 2D nanosheets. Avouris' group investigated the structure and electronic transport of graphene wrinkles generated on metallic substrates via atomic force microscopy.⁷³ The distinct electronic structure and charges in transport and diffusion were affiliated with various types of wrinkles on graphene. For transport behaviors along and across a folded wrinkle, for example, the averaged resistance along the folded wrinkle was found to be smaller than that across it. This anisotropy may be caused by comprehensive effects of diffusion of charges distributed across the multilayered folds versus local interlayer tunneling across the collapsed region ([Figure 4F](#)). Cui's group investigated wrinkles formed on a MoS₂ nanosheet during Li-ion intercalation because of volume expansion and a consequent strain. They suggested that Li-ion interlayer intercalation significantly enhances the electrical conductance and rate performance.⁷⁷

Plane-like Geometric Sites in 2D Materials

For a monolayer nanosheet with only one facet exposed, lithium/sodium-ion adsorption may play an important role for energy storage, and for layered 2D materials, lithium/sodium-ion intercalation between layers also matters for the electrochemical performance. Enlarging the interlayer spacings of layered 2D nanosheets, which we define as plane-like geometric sites in them, not only reduces the transport barrier and facilitates diffusion and storage of lithium/sodium ions, electrons, and mass, leading to improvement of electrochemical performance, but also relaxes the strain and buffers the volume expansion, thus enhancing the cycling stability. Heteroatom doping, small molecules, and particle intercalation are the most effective strategies to enlarge the interlayer spacings of layered materials.⁷⁸ As reported, the interlayer spacing of a pure few-layered graphene is 0.34 nm. Such graphene has widely been investigated as an anode material in LIBs and has revealed superior electrochemical performance, as we discussed above (~1,200 mAh g⁻¹ at 100 mA g⁻¹). However, sodium ions with a larger radius could not easily intercalate it, thus restricting the application of Na-ion batteries (~200 mAh g⁻¹ at 50 mA g⁻¹). Our group investigated the Na-ion storage of heteroatom-doped few-layered graphene with different interlayer spacings (nitrogen-doped graphene, 0.34 nm; phosphorus-doped graphene, 0.40 nm).³⁷ Based on DFT calculations, a phosphorus-doped bilayer graphene can accommodate 19 sodium ions, while a nitrogen-doped bilayer graphene could accommodate 10 sodium ions, which apparently contribute to the capacity ([Figure 5A](#)). The experimental data also confirmed that phosphorus-doped graphene delivers an ultrahigh reversible capacity of 374 mAh g⁻¹ after 120 cycles at 25 mA g⁻¹, while nitrogen-doped graphene exhibits a slight decay and a relatively low capacity (211 mAh g⁻¹) after 50 cycles. Expanding interlayer spacings has also been utilized to enhance the energy storage of layered MoS₂ nanosheets. Cui's group continuously controlled interlayer spacings of vertically aligned MoS₂ nanosheets via electrochemical intercalation of Li ions into van der Waals gaps and

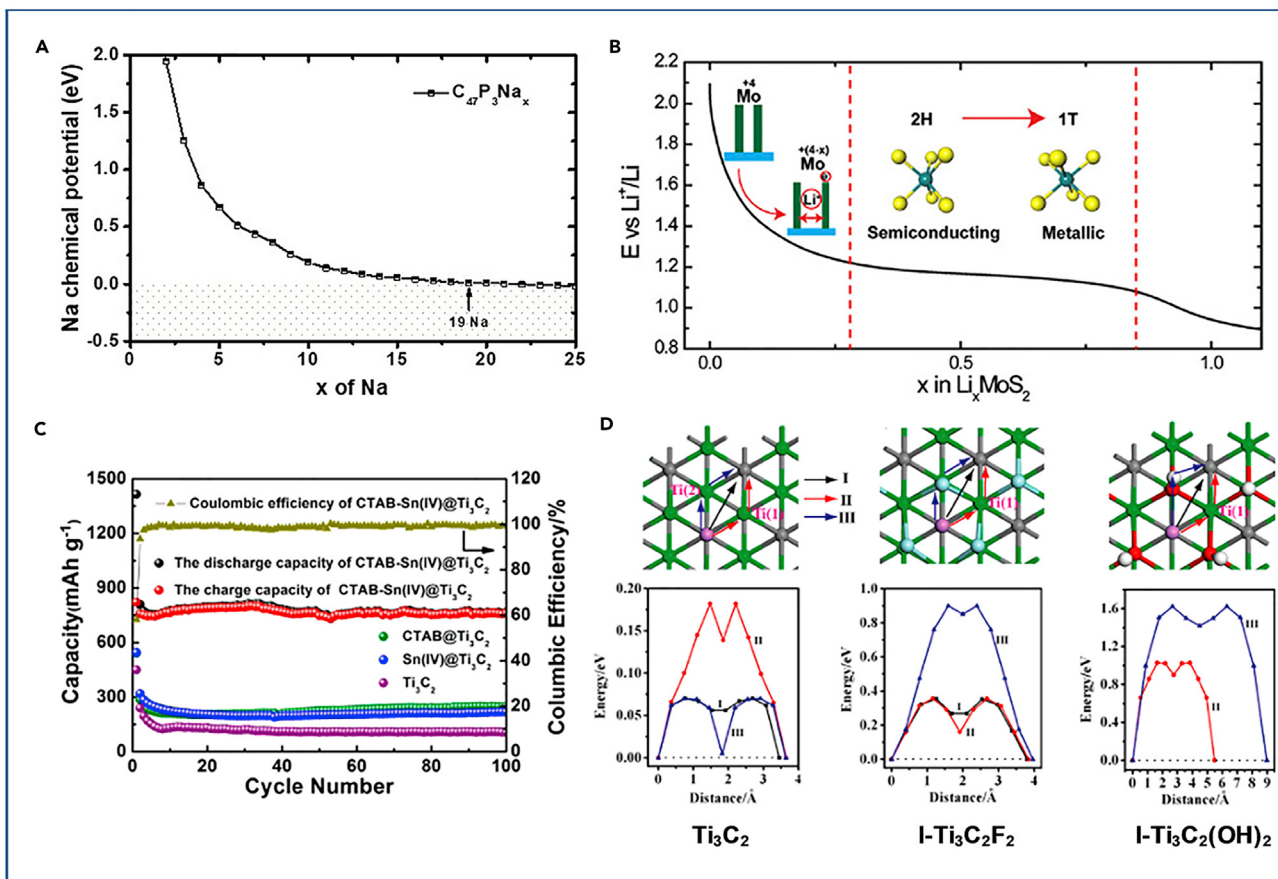


Figure 5. Plane-like Geometric Sites of 2D Materials for Rechargeable Batteries

(A) Chemical potential as a function of number of sodium ions based on DFT calculations. Reproduced from Yang et al.,³⁷ with permission.
(B) Galvanostatic discharge curve under corresponding lithiation process. Lithium ions intercalate into the interlayer of MoS₂, leading to the expansion of the interlayer spacing. Reproduced from Wang et al.,⁷⁹ with permission.
(C) Cycling performances of Ti₃C₂, CTAB@Ti₃C₂, Sn(IV)@Ti₃C₂, and CTAB-Sn(IV)@Ti₃C₂ at 100 mA g⁻¹. Reproduced from Luo et al.,⁸¹ with permission.
(D) Schematic illustrations of lithium-ion diffusion paths and their corresponding diffusion barrier profiles of lithium ion on Ti₃C₂, I-Ti₃C₂F₂, and I-Ti₃C₂(OH)₂. Reproduced from Tang et al.,⁸² with permission.

studied the relationship of voltage of Li⁺/Li and interlayer spacings (Figure 5B).⁷⁹ Liu et al.⁸⁰ reported the preparation of restacked MoS₂ nanosheets along the c axis via an exfoliation and restacking process. The restacked MoS₂ nanosheets exhibited an enhanced reversible capacity of 800 mAh g⁻¹ in the first charge at the current density of 50 mA g⁻¹, and maintained a capacity of 750 mAh g⁻¹ after 20 cycles.

Transition metal carbides, carbonitrides and nitrides (termed MXenes), are the latest composite materials to join the 2D materials family, and represent a rapid development in the energy-storage field.^{83,84} Tao et al.⁸¹ fabricated pillar-structured Ti₃C₂ MXene 2D materials via a liquid-phase cetyltrimethyl-ammonium bromide (CTAB) prepillaring and Sn⁴⁺ pillaring method. The interlayer spacing of Ti₃C₂ MXene nanosheets (CTAB-Sn(IV)@Ti₃C₂) can be tuned based on the size of the intercalated prepillaring agent and can reach 2.230 nm (CTAB@Ti₃C₂, 40°C) compared with the pristine interlayer spacing of 0.977 nm. Because of the pillar effect, the layered CTAB-Sn(IV)@Ti₃C₂ nanosheets deliver a highly reversible capacity of 765 mAh g⁻¹ after 100 cycles at 100 mA g⁻¹, which is higher than those of Sn(IV)@Ti₃C₂ (218 mAh g⁻¹) and CTAB@Ti₃C₂ (248 mAh g⁻¹), thus confirming the excellent electrochemical performance (Figure 5C).

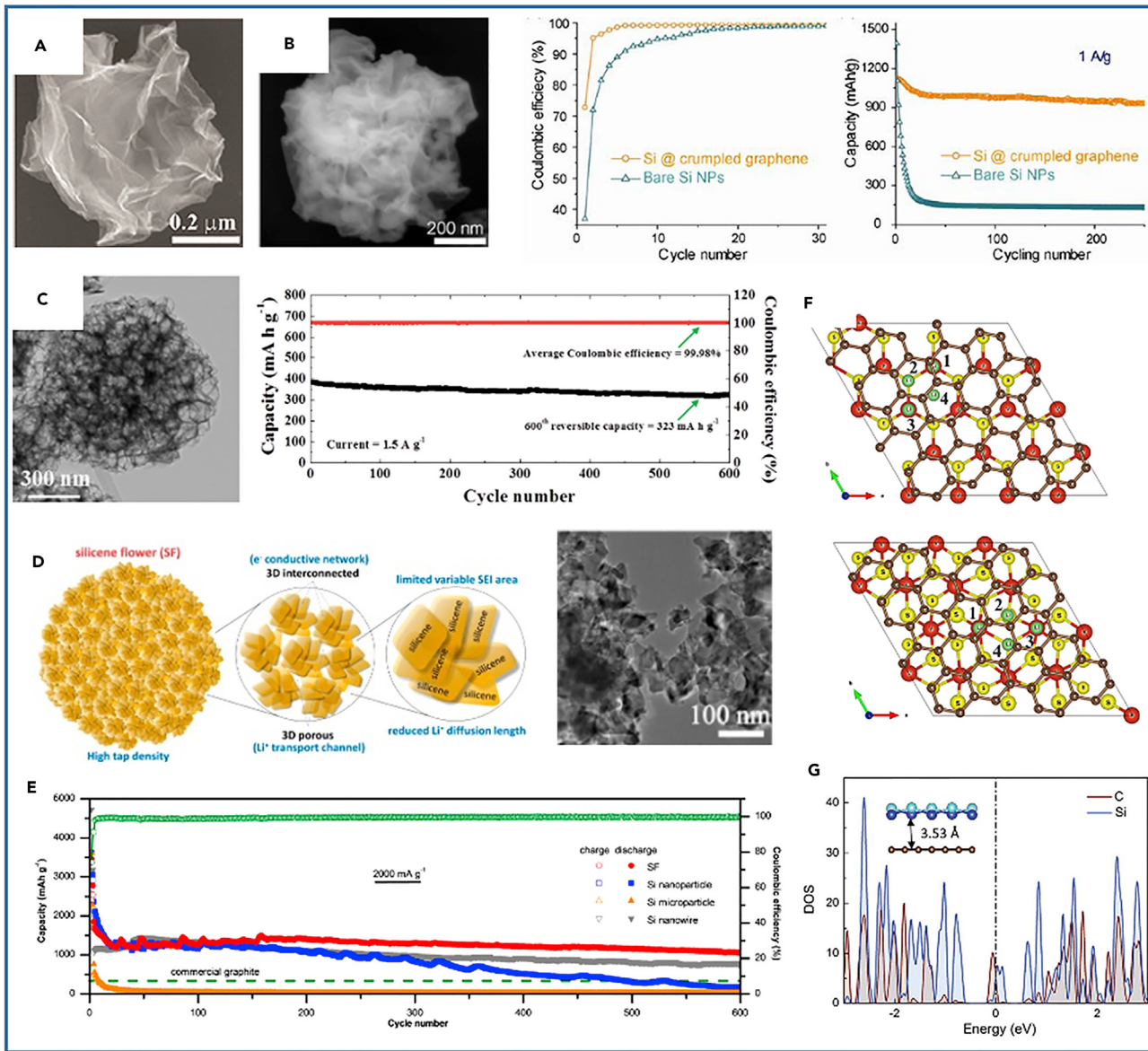
Besides the interlayer spacing, the surface structure is also of great importance to the electrochemical performance. Taking MXene nanosheet with various surface terminations (hydroxyl, oxygen, or fluorine) as an example, a Ti_3C_2 monolayer and its F- and OH-functionalized forms, and their potentials for battery anodes, were investigated via DFT calculations (Figure 5D).⁸² Ti_3C_2 , $\text{Ti}_3\text{C}_2\text{F}_2$, and $\text{Ti}_3\text{C}_2(\text{OH})_2$ monolayers with 2×2 supercell can accommodate up to eight, four, and two Li ions, respectively. For a Ti_3C_2 monolayer, the Li-ion diffusion barrier (top C \rightarrow top C or top C \rightarrow top Ti) is about 0.07 eV with diffusion path lengths of 0.762 and 0.727 Å. For the $\text{Ti}_3\text{C}_2\text{F}_2$ and $\text{Ti}_3\text{C}_2(\text{OH})_2$ monolayers, the Li ions diffuse through C \rightarrow Ti \rightarrow C (energy barriers of 0.27 and 1.07 eV, respectively) instead of C \rightarrow C, which could be attributed to the steric effects, suggesting that the bare Ti_3C_2 monolayer exhibits the best electrical conductivity, low diffusion barrier, and the highest theoretical capacity compared with $\text{Ti}_3\text{C}_2\text{F}_2$ and $\text{Ti}_3\text{C}_2(\text{OH})_2$ derivatives. Besides DFT calculations, the experimental measurements were conducted by Kent and co-workers.⁸⁵ They tried to remove the surface groups by annealing and investigated the lithium storage in Ti_3C_2 nanosheets with remnant O groups via *in situ* X-ray adsorption spectroscopy and inelastic neutron scattering. These studies suggested that extra Li layers can be formed on the surfaces of lithiated O-terminated Ti_3C_2 nanosheets (with high specific surfaces) to accommodate more Li ions, thus leading to higher capacity.

In brief, the point-like geometric sites on 2D materials, such as heteroatom doping and vacancies, could increase the number of active sites to accommodate or react with more guest ions (such as Li^+ and Na^+), thus improving the capacity. The line-like geometric sites (such as edges, zigzag/armchair directions, or wrinkles of 2D materials) significantly lower the energy barrier of 2D materials and facilitate the Li/Na diffusions. In plane-like geometric sites, enlarged interlayer spacing not only reduces the transport barrier and facilitates ionic/electronic transport, but also relaxes the strain and buffers the volume expansion, thus finally enhancing the total electrochemical performance. In addition, the geometric sites on 2D materials also provide benefit to other energy-storage devices. For example, a N-doped graphene-based supercapacitor exhibits 4-fold larger capacitance than the pristine graphene-based counterpart.⁸⁶ The graphitic and pyridinic nitrogen atoms could lead to enhanced wettability of doped graphene because of their large dipole moments, while graphitic nitrogen of doped graphene promotes the electron transfer, thus improving the capacitive performance because of lower charge-transfer resistance. Nitrogen-doped graphene was also utilized to improve the electrochemical behavior due to introduction of the active site by nitrogen doping.⁸⁷

Hierarchical Geometric Structures from 2D Materials

In addition to nanogeometric sites within 2D materials, mesogeometric structures, built from 2D materials, also play vital roles in the enhanced electrochemical performance of lithium/sodium-ion batteries. Constructing hierarchical structures from 2D nanosheets enables novel chemical, physical, or mechanical functionalities, and consequently buffers the volumetric expansion. In this section, we aim at summarizing 2D material utilization toward creation of various hierarchical architectures for rechargeable batteries.

Crumpled particles obtained from single nanosheets are the popular object for building a 3D structure. Huang's group fabricated crumpled graphene oxide (GO) by capillary compression in rapidly evaporating aerosol droplets of GO. In a droplet of GO, the surface tension acts as the main driving force that makes a GO nanosheet compress and irreversibly crumple into a 3D nanoparticle when the droplet radius

**Figure 6. Hierarchical Geometric Structures from 2D Materials**

- (A) A crumpled graphene particle via rapid isotropic compression in evaporating aerosol droplets. Reproduced from Luo et al.,⁸⁸ with permission.
(B) Scanning electron microscopic image of Si nanoparticles@crumpled graphene and its electrochemical performances. Reproduced from Luo et al.,⁸⁹ with permission.
(C) Morphologies of the 3D MoS₂-graphene composite microspheres and their cycling performance. Reproduced from Choi et al.,⁴⁰ with permission.
(D) Schematic illustration of a silicene flower with hierarchical structure and its TEM image. Reproduced from Zhang et al.,⁹¹ with permission.
(E) The electrochemical performance of silicene flowers. Reproduced from Zhang et al.,⁹¹ with permission.
(F) Lithium ion sites on a VS₂/graphene heterostructure. Reproduced from Mikhaleva et al.,⁹² with permission.
(G) The density of states of a silicene/graphene heterostructure. Reproduced from Shi et al.,⁹³ with permission.

decreases during evaporation (Figure 6A).⁸⁸ The same group further encapsulated silicon nanoparticles into crumpled GO nanoparticles and utilized the obtained 3D Si@GO materials as anodes for LIBs (Figure 6B).⁸⁹ The 3D Si@GO GO not only doubled the coulombic efficiency of Si nanoparticles (73% Si@GO vs. 37% of Si) at a current density of 1,000 mA g⁻¹, but also improved the cycling stability and maintained a reversible capacity of 940 mAh g⁻¹ after 250 cycles, since the crumpled GO

shell prevented Si nanoparticles from the electrolyte solvents and buffered the volume expansion without cracking. Kang's group reported that the synthesis of 3D MoS₂-graphene microspheres consisted of dozens of uniform crumpled graphene nanospheres coated with few-layered MoS₂ using a spray pyrolysis process.⁴⁰ The obtained 3D MoS₂-graphene delivered superior Na-ion storage properties: a high capacity of 797 mAh g⁻¹ at a current density of 200 mA g⁻¹ during the first cycle, 323 mAh g⁻¹ at a current density of 1,500 mA g⁻¹, high coulombic efficiency of 99.98% during the 600 cycles. Such properties may be attributed to the 3D structure of the crumpled microspheres, which offered voids for volume expansion and pathways for a fast electron transfer during sodiation (Figure 6C). Lou et al.⁹⁰ demonstrated the preparation of 3D MoS₂ microflowers composed of ultrathin nanosheets with the assistance of a polystyrene microsphere template. The as-prepared hierarchical structures delivered a reversible capacity of 585 mAh g⁻¹ after 50 cycles at a current density of 100 mA g⁻¹, which was much better than that of MoS₂ nanoflakes (163 mAh g⁻¹ after 50 cycles).

Silicene microflowers composed of inherently interconnected silicene nanosheets with anisotropic orientations were fabricated and utilized as the anode materials for LIBs. The 3D flower-like ensembles exhibited excellent electrochemical performance (Figure 6D), including high gravimetric capacity (2000 mAh g⁻¹ at 800 mA g⁻¹), superior volumetric capacity (1700 mAh cm⁻³), extraordinary rate performance (950 mAh g⁻¹ at 8,000 mA g⁻¹), and perfect cycling stability (1,100 mAh g⁻¹ after 600 cycles at the current density of 2,000 mA g⁻¹), as shown in Figure 6E.⁹¹ The silicene nanoplates in the building stacks were interconnected in spatial directions, which could accommodate the volume expansion of Si during cycling, ensure the structural stability, lead to the formation of non-variable solid-electrolyte interface (SEI), improve the interfacial stability, and shorten the Li-ion diffusion length and electron transport paths within the building blocks.

Hierarchically layered structures made of 2D materials mainly include 0D-2D, 1D-2D, and 2D-2D hybrid composites. We herein focus on 2D-2D stacked heterostructures, which are also called van der Waals heterostructures. Such heterostructures are formed through stacking of different atomic layers, layer by layer, which controls and manipulates the generation and diffusion of Li/Na ions and electrons within the atomic interfaces and facilitates the improvement of energy storage. So far there have been only a few reports on van der Waals heterostructures utilized for energy storage because of poorly developed fabrication processes. Mikhaleva et al. simulated Li-ion adsorption and diffusion on the surface and in the interlayer spacings of VS₂ monolayer/graphene van der Waals heterostructures by DFT calculations (Figure 6F).⁹² The maximum amount of ions accommodated on the surface and within interlayers of layered VS₂/graphene heterostructures gave the general formula of Li/VS₂/Li_{1.75}/C_{0.35}/Li_{0.583}. The overall capacity was calculated as 569 mAh g⁻¹, which is much higher than that of a VS₂ monolayer (466 mAh g⁻¹). Shi et al. predicted the electrochemical performance of silicene/graphene van der Waals heterostructured anodes for Li/Na-ion batteries.⁹³ DFT calculations showed that the Si/G heterostructures not only exhibit excellent electrochemical properties, including high lithium/sodium capacity (487 mAh g⁻¹) and low lithium/sodium diffusion barriers (<0.4 eV for lithium and <0.3 eV for sodium, respectively), but also maintain their metallic properties before and after ion intercalation (Figure 6G), ensuring good rate capabilities. Furthermore, the mechanical strength of the Si/G heterostructures was calculated to be larger than that of pure silicene or graphene, thus buffering the volume expansion, preserving the structural integrity during lithiation/sodiation, and enhancing the cycling stability.

Real-Time Observations of Geometric Storage Mechanism

As already discussed, creating various defects (point-, line-, and plane-like geometric sites) in 2D materials is an effective strategy to expand their energy storage. Constructing 3D hierarchical materials from 2D nanosheets is also proven as a beneficial route toward better electrochemical properties. However, the issues of how the geometry works on improving the lithium/sodium-ion storage and its implementation in relation to the energy-storage mechanisms have not been well divulged. Various *in situ* techniques, such as *in situ* neutron studies, *in situ* X-ray diffraction, *in situ* Raman spectroscopy, *in situ* Fourier transform infrared spectroscopy, *in situ* nuclear magnetic resonance, *in situ* X-ray adsorption spectroscopy, *in situ* TEM, and *in situ* atomic force microscopy, have been developed to investigate material structural evolutions, the dynamic process of electrochemical reactions, and electrode/electrolyte phase/interface change mechanisms during operation. Up to now, most of the *in situ* techniques could only provide real-time investigation of structural evolution at macroscopic and statistical scale, whereby only *in situ* TEM is extensively utilized in studying lithium/sodium-ion storage mechanisms at the atomic scale since the first nanobattery utilizing a single SnO₂ nanowire was constructed by Huang and co-workers.^{94,95} *In situ* TEM has been proved to be a powerful technique to not only directly visualize the microstructural transformation and Li/Na-ion diffusion at the atomic scale but also to probe the electrochemical reactions during charge/discharge processes.^{96–99} Besides direct visualization of morphology changes, the electrochemical reactions between the electrode materials and lithium/sodium metals can be detected by lattice image alternations, real-time selected area electron diffraction, electron energy loss spectroscopy, and energy-dispersive X-ray spectroscopy (EDS). For instance, our group constructed a nanobattery composed of a single nitrogen-doped graphene nanosheet attached to a golden wire as the anode, a piece of lithium metal adhered to a tungsten wire as the cathode, and an ionic liquid as the electrolyte (Figure 7A). Based on the real-time observations, we confirmed the existence of the ordered sp² honeycomb carbon lattices and disordered domains at the nitrogen substitution sites before lithiation. After lithiation, two types of SEI films were observed on the ordered and disordered areas in graphene nanosheet, and more disordered defects formed on nitrogen sites, suggesting that they exhibit much more active properties (Figure 7B).⁶¹ The expansion of interlayer spacing of layered phosphorus-doped graphene during the first sodiation cycle and reversible changes of interlayer distance during the following charge/discharge processes were visualized under *in situ* TEM, suggesting that sodium ions can reversibly intercalate/deintercalate into/out of the graphene interlayers, and uncovering the reasons for enhanced capacity and long cycling stability (Figure 7C).³⁷ Cui's group investigated the sodiation mechanism of hybrid materials composed of a phosphorene nanosheet sandwiched between graphenes. The latter delivered a high specific capacity of 2,440 mAh g⁻¹ at the current density of 50 mA g⁻¹ and a superior cycling stability, 83% capacity retention after 100 cycles. The *in situ* TEM images showed that the phosphorene layer exhibits about 92% volume expansion along the y axis while the nanosheet along the x axis shows inconspicuous change, which may result from the anisotropic diffusion of sodium ions along x and y axes (Figure 7D). The graphene layers sandwiched between phosphorene nanosheets work as a mechanical backbone to accommodate the volume expansion, which is also proved by *in situ* TEM.²² Zeng et al. reported the real-time observation of lithiation-induced structural expansion and deformation of MoS₂ nanosheet anodes in a LiPF₆/EC/DEC electrolyte during lithiation/delithiation using *in situ* liquid cell TEM (Figure 7E).¹⁰⁰ During the first lithiation, more than 50% of MoS₂ nanosheets decomposed irreversibly at a voltage of 0.81.2 V, leading to the formation of MoS₂ nanoparticles of 5–10 nm in

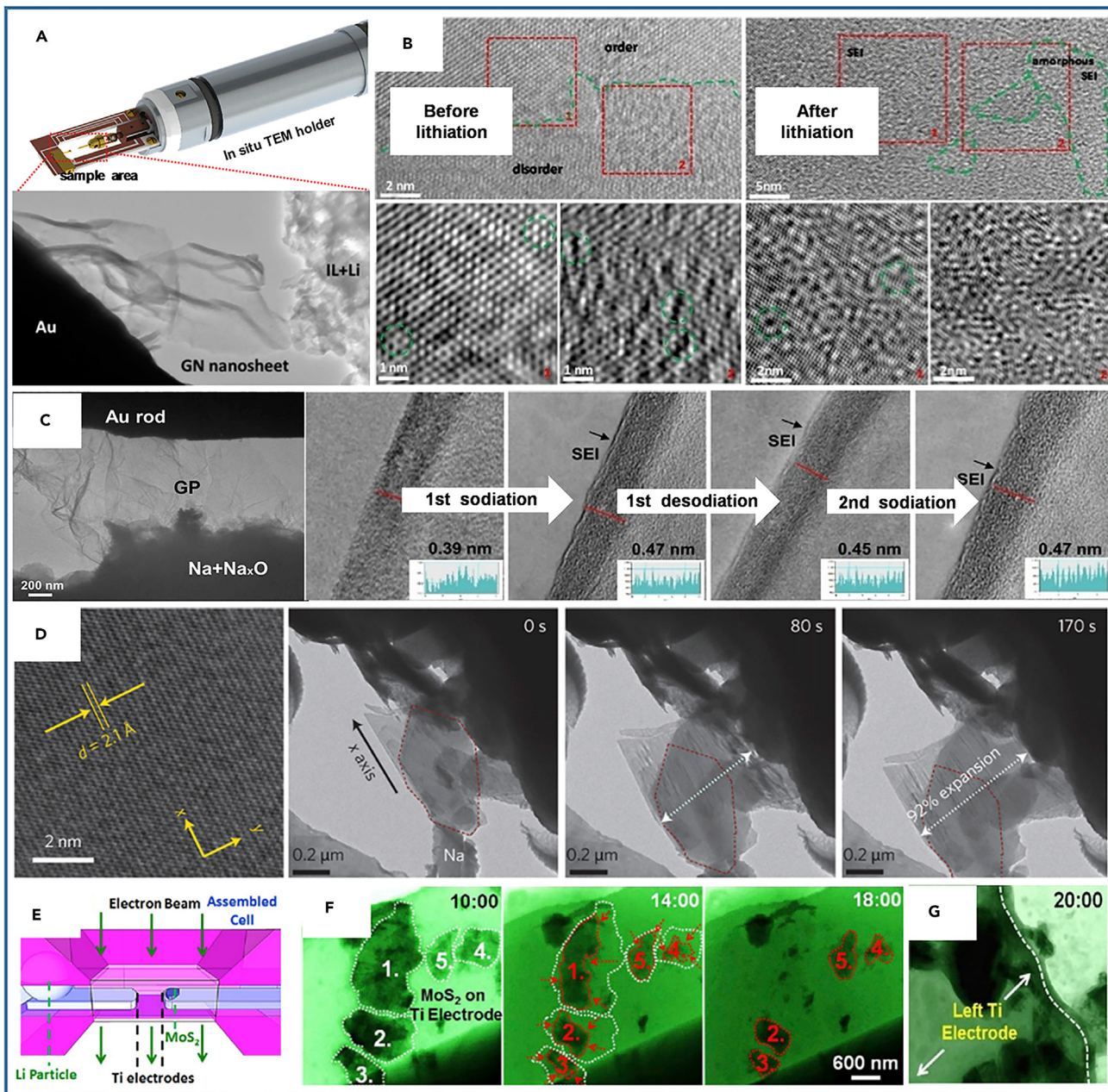


Figure 7. Application of *In Situ* TEM for 2D Materials Electrodes

- (A) Schematic illustration of *in situ* TEM holder and a nanobattery containing the nitrogen-doped graphene. Reproduced from Wang et al.,⁶¹ with permission.
- (B) HRTEM images of basal plane structure evolution of nitrogen-doped graphene before and after lithiation. The green dashed line in the upper left image differentiates the ordered and disordered domains of GN, while the green dashed line in the upper right image suggests the existence of amorphous SEI. The green circles in the lower images (from left to right) represent some dislocations, hole defect sites in GN, and some dislocations in the SEI layer, respectively. Reproduced from Wang et al.,⁶¹ with permission.
- (C) TEM image of a nanobattery with a phosphorus-doped graphene anode and the structural evolution of the GP edge during the charge/discharge processes. Reproduced from Yang et al.,³⁷ with permission.
- (D) Real-time observation of morphology evolution of black phosphorus/graphene hybrid. One black phosphorus particle is marked by red dashed line to visualize the anisotropic morphology evolution (x axis versus y axis) during the potentiostatic sodiation. Reproduced from Sun et al.,²² with permission.
- (E) The window area in an electrochemical liquid cell. Reproduced from Zeng et al.,¹⁰⁰ with permission.
- (F) *In situ* electrochemical reaction of MoS₂ nanosheets with LiPF₆/EC/DEC electrolyte in a liquid cell. Reproduced from Zeng et al.,¹⁰⁰ with permission.
- (G) The formation of SEI on the left-hand-side Ti electrode. Reproduced from Zeng et al.,¹⁰⁰ with permission.

size in less than 5 s (Figure 7F). An SEI layer was also discerned on the anode side of the titanium electrode adhered to lithium metal. The SEI layer was 200 nm thick and composed of LiF nanocrystals containing C and O, as confirmed by EDS (Figure 7G). Such *in situ* TEM techniques pave the way toward direct visualization of electrochemical performance of 2D electrode materials and battery degradation mechanisms. Even so, the *in situ* TEM technique still faces some challenges that need to be addressed. As we mentioned above, the nanobatteries constructed by Li₂O/Li system or liquid cell are incapable of completely simulating real battery-operation conditions. For example, the formation of SEI layers (Li₂O layer) can be visualized in real time through *in situ* TEM, but the practically used electrolyte can barely be applied under such conditions. Notably, the real process is highly dependent on each particular electrolyte, which cannot be well observed at present.

Conclusions and Perspective

Studying energy storage in geometric sites is an emerging research direction that is attracting increasing attention with respect to improving the specific capacity and discovering new energy-storage mechanisms. The constructions of new geometric sites on inner- or intra-channels of 2D layered materials offer new options to address the challenges arising from lower energy density and sluggish Li transport kinetics. This article reviewed the progress in regard of point-, line-, and plane-like geometric sites for lithium/sodium-ion storage. These include in-plane and out-plane sites in a 2D material, hierarchical structures made from 2D materials, and the corresponding *in situ* TEM mechanism investigations. This review can direct the further 2D layered materials design, and their fabrication and utilization in advanced lithium/sodium-ion storage devices. Despite the significant progress made in this field, there are still some challenges that remain to be timely addressed:

Applications of Geometry Concept for Materials Design

The past years have witnessed great progress in utilizing 2D materials on lithium/sodium-ion storage and the rapid development of geometry-driven energy storage of 2D materials. These reported materials exhibited a commonality of structural features that can be indexed within a given geometric model. The introduction of geometry into materials design would greatly accelerate the development of advanced battery electrodes. The crucial task for geometry materials design is the intelligent screening of effective sites for guest-ion storage and adoption of the derived geometry concepts for materials design. The deep integration of material design and geometry, and high-throughput syntheses of electrode materials with certain geometric sites are required to promote future developments. In addition, this design philosophy is believed to aid development of the catalysis area, for example, to create such novel and powerful single-atom catalysts (SACs), single-molecular catalysts (SMCs), and multiple-component SACs and SMCs. Specifically, we believe that various fields (e.g., electric, magnetic, light, stress) that involve SAC and SMC catalysts or electrodes (such as magnetic catalysts and magnetic electrodes) offer dramatic promise, whereby atomic/molecular energy or momentum can be added. These concepts should be realized in the geometric sites in 2D materials.

Challenges of Mass Production and Cost Analysis

2D materials with geometric sites promise enhanced performance in energy and power densities of energy-storage systems. However, concerning the practical applications, great challenges still exist and need to be overcome. First and foremost, the innovative materials should be produced on a large scale. Many reports of 2D materials in lithium/sodium-ion storage are based on laboratory experiments and theoretical calculations. Generally, the fundamental research usually conducted

on the laboratory scale ignores the cost and production scale. To close this gap, the main task is to focus on the fabrication method and the raw materials. Extreme synthetic conditions should be avoided if possible. For example, what is accessible for the ultrahigh pressure or temperature in the laboratory may be impossible for mass production. Therefore, mild reaction conditions should draw increased attention. Second, the inexpensiveness of raw materials is also another critical benefit in decreasing the overall cost. Technological breakthroughs and, eventually, practical applications can be anticipated through continuous academic progress in both of these aspects. Last but not least, 2D materials themselves, with high specific surface area, exhibit relatively low volumetric capacity compared with their bulk counterparts. The restack and elongation of 2D materials during battery operation also damage their cycle life. In addition, the large surface area of 2D materials leads to the successive formation of an SEI layer, which could passivate the active sites and result in inferior electrochemical performance. The introduction of geometric sites into 2D materials, such as protrusion, enlarged interlayer spacing, and crumpled geometric structures, may also lower the volumetric density while at the same time creating new storage sites for guest ions. How to balance the opposite effects of geometric sites on 2D materials is still to be further investigated, such as the manufacture of 3D dense structures assembled by 2D structures.

Theoretical Calculations for Performance Prediction

Theoretical calculations disclose how the guest ions are stored in the geometric sites and point out the stable configuration after ion insertion. This could explain extra capacity beyond the theoretical values based on the insertion/conversion mechanism. Theoretical calculations combined with the discussed geometric concept would unambiguously predict the electrochemical performance.

In Situ Techniques for Mechanism Investigations

The rapid development of *in situ* electrochemical techniques, and especially the corresponding *in situ* cell studies, provides direct evidence through observing the electrodes during battery cycling, which has brought new fundamental understanding of lithium/sodium-ion storage mechanisms. The described *in situ* research is mainly conducted under TEM. The multi-mode *in situ* techniques, which include *in situ* X-ray and other spectroscopy techniques, should also be introduced to monitor the evolution of geometric sites during ion insertion/desertion.

It can be expected that the rapidly developing field of geometric-site-related lithium/sodium-ion storage will bring about more advanced 2D layered energy-storage materials. Certainly this would be highly dependent on the integration of material geometry, material science, electrochemistry, and battery engineering techniques. The upcoming progress will gather together materials scientists, chemists, and mathematicians to develop high-performance energy-storage materials with special defect geometry for advanced rechargeable batteries.

Experimental Procedures

The electronic properties and DOS of defective graphene and MoS₂ are calculated by the DFT implemented in the Vienna *ab initio* simulation package (VASP),^{101,102} in which the projected augmented wave method^{103,104} and the Perdew-Burke-Ernzerhof exchange correlation are used.¹⁰⁵

For the mono- and divacancy and S-vacancy MoS₂, we use a 5 × 5 × 1 hexagonal supercell of graphene and MoS₂. For the line-defective graphene, we use a 2 × 15 × 1 rectangular supercell. Similarly, we built two rectangular supercells for

the zigzag and armchair nanoribbons of MoS₂, containing 35 and 36 atoms, respectively.

The Monkhorst-Pack scheme of k-mesh is used. For details, a $7 \times 7 \times 1$ k-mesh is used for the mono- and divacancy and S-vacancy MoS₂, a $2 \times 15 \times 1$ k-mesh for the line-defective graphene, and a $10 \times 1 \times 1$ k-mesh for zigzag, along with a $1 \times 10 \times 1$ k-mesh for armchair defect of MoS₂. The cutoff energy is 520 eV for the graphene systems and 400 eV for the MoS₂ ones.

The geometric structures of all systems are firstly used with a force threshold of 0.02 eV Å⁻¹. The DOS and the charge density of the defective states are then calculated.

ACKNOWLEDGMENTS

X.W. appreciates the support from "the Fundamental Research Funds for the Central Universities" (no. 2016RC008), the "1000 Youth Talent plan" project, and the "Excellent One Hundred" project of Beijing Jiaotong University. Y.Y. acknowledges financial support from "the Fundamental Research Funds for the Central Universities" (no. 2017JBM068). X.L. acknowledges financial support from the National Natural Science Foundation of China (no. 21603162). D.G. is grateful to the Australian Research Council (ARC) for granting a Laureate Fellowship (project no. FL160100089) and QUT grant 322120-0355/51.

AUTHOR CONTRIBUTIONS

Conceptualization, X.W., Y.B., J.Y., and D.G.; Investigation, Y.Y. and X.L.; Resources, Y.Y., X.L., Y.Z., and Z.Z.; Writing – Original Draft, Y.Y. and X.L.; Writing – Review & Editing, Y.Y., X.W., and D.G.; Supervision, Y.B., J.Y., D.G., and X.W.

REFERENCES

1. Suss, M.E., and Presser, V. (2018). Water desalination with energy storage electrode materials. *Joule* 2, 10–15.
2. Armand, M., and Tarascon, J.M. (2008). Building better batteries. *Nature* 451, 652–657.
3. Gao, W., Singh, N., Song, L., Liu, Z., Reddy, A.L.M., Ci, L., Vajtai, R., Zhang, Q., Wei, B., and Ajayan, P.M. (2011). Direct laser writing of micro-supercapacitors on hydrated graphite oxide films. *Nat. Nanotech.* 6, 496–500.
4. Chen, Z., Ren, W., Gao, L., Liu, B., Pei, S., and Cheng, H.-M. (2011). Three-dimensional flexible and conductive interconnected graphene networks grown by chemical vapour deposition. *Nat. Mater.* 10, 424–428.
5. Olivetti, E.A., Ceder, G., Gaustad, G.G., and Fu, X. (2017). Lithium-ion battery supply chain considerations: analysis of potential bottlenecks in critical metals. *Joule* 1, 229–243.
6. Hou, G., Cheng, B., Cao, Y., Yao, M., Li, B., Zhang, C., Weng, Q., Wang, X., Bando, Y., Golberg, D., and Yuan, F. (2016). Scalable production of 3D plum-pudding-like Si/C spheres: towards practical application in Li-ion batteries. *Nano Energy* 24, 111–120.
7. Dong, J., Xue, Y., Zhang, C., Weng, Q., Dai, P., Yang, Y., Zhou, M., Li, C., Cui, Q., Kang, X., et al. (2017). Improved Li⁺ storage through homogeneous N-doping within highly branched tubular graphitic foam. *Adv. Mater.* 29, 1603692.
8. Bonaccorso, F., Colombo, L., Yu, G., Stoller, M., Tozzini, V., Ferrari, A.C., Ruoff, R.S., and Pellegrini, V. (2015). Graphene, related two-dimensional crystals, and hybrid systems for energy conversion and storage. *Science* 347, 1246501.
9. Raccichini, R., Varzi, A., Passerini, S., and Scrosati, B. (2014). The role of graphene for electrochemical energy storage. *Nat. Mater.* 14, 271.
10. Kucinskis, G., Bajars, G., and Kleperis, J. (2013). Graphene in lithium ion battery cathode materials: a review. *J. Power Sources* 240, 66–79.
11. Vargas, C.O.A., Caballero, A., and Morales, J. (2012). Can the performance of graphene nanosheets for lithium storage in Li-ion batteries be predicted? *Nanoscale* 4, 2083–2092.
12. Wang, Y.-X., Chou, S.-L., Liu, H.-K., and Dou, S.-X. (2013). Reduced graphene oxide with superior cycling stability and rate capability for sodium storage. *Carbon* 57, 202–208.
13. Xu, J., Dou, Y., Wei, Z., Ma, J., Deng, Y., Li, Y., Liu, H., and Dou, S. (2017). Recent progress in graphite intercalation compounds for rechargeable metal (Li, Na, K, Al)-ion batteries. *Adv. Sci.* 4, 1700146.
14. Tan, C., and Zhang, H. (2015). Two-dimensional transition metal dichalcogenide nanosheet-based composites. *Chem. Soc. Rev.* 44, 2713–2731.
15. Chhowalla, M., Liu, Z., and Zhang, H. (2015). Two-dimensional transition metal dichalcogenide (TMD) nanosheets. *Chem. Soc. Rev.* 44, 2584–2586.
16. Chhowalla, M., Shin, H.S., Eda, G., Li, L.-J., Loh, K.P., and Zhang, H. (2013). The chemistry of two-dimensional layered transition metal dichalcogenide nanosheets. *Nat. Chem.* 5, 263.
17. Zhou, J., Qin, J., Zhang, X., Shi, C., Liu, E., Li, J., Zhao, N., and He, C. (2015). 2D space-confined synthesis of few-layer MoS₂ anchored on carbon nanosheet for lithium-ion battery anode. *ACS Nano* 9, 3837–3848.
18. Qie, L., Chen, W.-M., Wang, Z.-H., Shao, Q.-G., Li, X., Yuan, L.-X., Hu, X.-L., Zhang, W.-X., and Huang, Y.-H. (2012). Nitrogen-doped porous carbon nanofiber webs as anodes for lithium ion batteries with a superhigh capacity and rate capability. *Adv. Mater.* 24, 2047–2050.
19. Duan, X., Xu, J., Wei, Z., Ma, J., Guo, S., Liu, H., and Dou, S. (2017). Atomically thin

99. Wang, X., Tang, D.-M., Li, H., Yi, W., Zhai, T., Bando, Y., and Golberg, D. (2012). Revealing the conversion mechanism of CuO nanowires during lithiation-delithiation by *in situ* transmission electron microscopy. *Chem. Commun.* 48, 4812–4814.
100. Zeng, Z., Zhang, X., Bustillo, K., Niu, K., Gammer, C., Xu, J., and Zheng, H. (2015). *In Situ* study of lithiation and delithiation of MoS₂ nanosheets using electrochemical liquid cell transmission electron microscopy. *Nano Lett.* 15, 5214–5220.
101. Kresse, G., and Hafner, J. (1993). Ab initio molecular dynamics for open-shell transition metals. *Phys. Rev. B* 48, 13115–13118.
102. Kresse, G., and Furthmüller, J. (1996). Efficiency of ab-initio total energy calculations for metals and semiconductors using a plane-wave basis set. *Comput. Mater. Sci.* 6, 15–50.
103. Blöchl, P.E. (1994). Projector augmented-wave method. *Phys. Rev. B* 50, 17953–17979.
104. Kresse, G., and Joubert, D. (1999). From ultrasoft pseudopotentials to the projector augmented-wave method. *Phys. Rev. B* 59, 1758–1775.
105. Perdew, J.P., Burke, K., and Ernzerhof, M. (1996). Generalized gradient approximation made simple. *Phys. Rev. Lett.* 77, 3865–3868.